

Change Detection Studies in Matang Mangrove Forest Area, Perak

Mahirah Jahari¹, S. Khairunniza-Bejo^{1*}, Abdul Rashid Mohamed Shariff¹,
Helmi Zulhaidi Mohd. Shafri²

¹*Department of Biological and Agricultural Engineering,*

²*Department of Civil Engineering, Faculty of Engineering,*

Universiti Putra Malaysia, 43400 UPM, Serdang,

Selangor, Malaysia

**E-mail: skbejo@eng.upm.edu.my*

ABSTRACT

In this research work, three different techniques of change detection were used to detect changes in forest areas. One of the techniques used a local similarity measure approach to detect changes. This new approach of change detection technique, which used mutual information to measure the similarity between two multi-temporal images, was developed based on correspondence of the pixel values, rather than the difference in their intensity. Pixels suffering any changes will be maximally dissimilar. The study was conducted using multi-temporal SPOT 5 satellite images, with the resolution of 10 m x 10 m on 5th August 2005 and 13th June 2007. The experimental results show that local mutual information provides more reliable results in detecting changes of the multi-temporal images containing different lighting condition compared to the image differencing and NDVI technique, specifically in areas with less plant growth. In addition, it can also overcome the problem on selecting the threshold value. Besides, the findings of this study have also shown that band 3, which is sensitive to vegetation biomass, gave the best result in detecting area of changes compared to the others.

Keywords: Change detection, forest, image differencing, local similarity, mutual information, NDVI

INTRODUCTION

Mangrove is an ecological term referring to a diverse aggregation of trees and shrubs that form dominant plant communities in tidal saline wetlands along sheltered coasts (Lee & Yeh, 2009). Mangroves provide a variety of ecological services for human beings, such as the protection of coasts from typhoon damage, pollutant absorption, and water purification (Howari *et al.*, 2009). They also function as habitats for diverse flora and fauna, including many rare species (Murray *et al.*, 2003; Sheridan & Hays, 2003; Liu *et al.*, 2008; Nagelkerken *et al.*, 2008). In December 2004, the world was shocked by the tsunami that hit parts of Asia. The scale of the 26 December 2004 Indian Ocean tsunami was almost unprecedented. Danielsen *et al.* (2005) stated that the force of the tsunami impact in Cuddalore District in Tamil Nadu, India, has completely destroyed parts of a village and removed sand spit that formerly blocked the river, especially at the river mouth. However, areas with mangroves and tree shelterbelts were significantly less damaged compared to other areas. Unfortunately, mangrove forests are dramatically declining in most areas worldwide (Conchedda *et al.*, 2008; Alongi, 2002; FAO, 2007). Towards the end of the twentieth century, scientific concern began to focus on the unprecedented loss of naturally occurring mangrove ecosystems around the world (Bosire *et al.*, 2008).

Received: 5 July 2010

Accepted: 24 October 2010

*Corresponding Author

Remote sensing technology could provide adequate tool for monitoring tropical forests (Lee & Yeh, 2009). Satellite imageries cover large forested regions that are often difficult to access. The increasing availability of remote sensing data and the fast evolution in the change detection techniques (Lu *et al.*, 2004) could help to monitor activities in the forest areas. The goal of change detection is to discern those areas on digital images that depict change features of interest (e.g. forest clearing or land-cover/land-use change) between two or more image dates (Hayes & Sader, 2001).

To date, many change detection techniques have been developed. These include image differencing and Normalized Difference Vegetation Index (NDVI). Image differencing is a simple approach of the change detection technique. It is done by subtracting a pair of spatially registered images taken on different dates. In fact, image differencing is a common change detection approach for forested and agricultural areas (Coppin & Bauer, 1994; Guild *et al.*, 2004). This method has been documented widely in change detection research (Hayes & Sader, 2001). Some researchers favour this particular method due to its accuracy, simplicity in computation, and ease in interpretation (Podeh, 2009). The histogram of the resulting image depicts a range of pixel values from negative to positive numbers, where those clustered around zero represent no change and those at either tail represent reflectance changes from one image date to the next (Jensen, 1996). Interpreting the distinguished images might be difficult to do because different input values could have the same result after subtraction and the original pixel value information is not retained (Guild *et al.*, 2004).

Normalized Differenced Vegetation Index (NDVI) presents the amount of photosynthesizing vegetation. The greater the amount, the brighter the pixel will be. The NDVI is calculated using spectral reflectance measurements acquired in the red and near-infrared regions. The NDVI algorithm subtracts the red reflectance values from the near infrared and divides it by the sum of the near-infrared and red bands. Thus, the NDVI itself varies between -1.0 and +1.0. The NDVI emphasizes on the differences in the spectral response of different features and reduces the impacts of topographic effects and illumination. The NDVI has been shown to be highly correlated with green biomass, crown closure, and leaf area index, among other vegetation parameters (Sader *et al.*, 2001).

Mutual information is normally used globally to find the similarity between two images. It has the advantage of measuring the similarity of the images when the images were taken from different modalities (Alberga, 2009). It has widely been used to register medical images (Inglada, 2002). In addition, mutual information is also used to measure the similarity of individual image points to detect changes in medical images. The use of local mutual information in detecting landslide is promising. However, it is only used to detect extensive landslides, where the area covered by the landslide region is also identified as the largest area among the other regions (Khairunniza-Bejo *et al.*, 2010). Therefore, the use of the local mutual information in an environmental change detection field is still limited, and this requires further investigation to be carried out.

STUDY AREA AND IMAGERY USED

Study Area

The Matang Mangrove Perak forest is located approximately between the latitudes of 4°49'22.98"N to 4°34'12.91"N and the longitudes of 100°33'22.14"E to 100°39'43.41"E. Images with the resolution of 10 m x 10 m taken from SPOT 5 dated 5 August 2005 and 13 June 2007 (*Fig. 1*) were used to detect the changes in the selected forest areas.

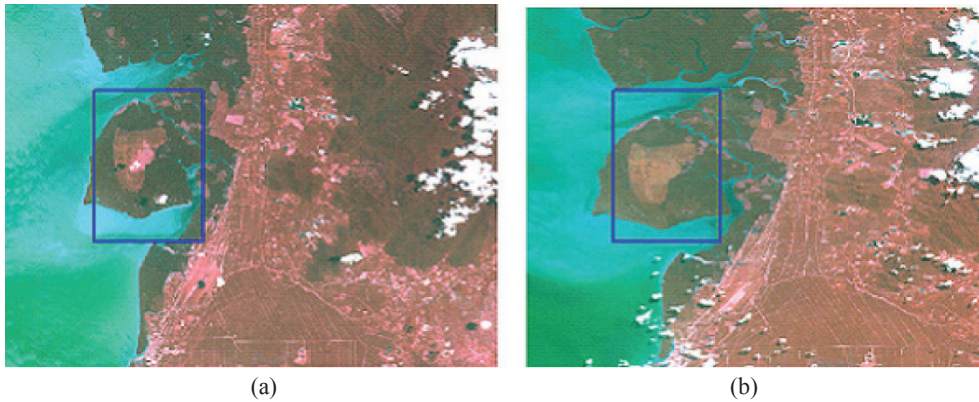


Fig. 1: Satellite image of Matang Mangrove Forest Area, Perak loaded with Bands 4, 3, and 2 taken from SPOT 5 (a) Image dated 5th August 2005, (b) Image dated 13th June 2007

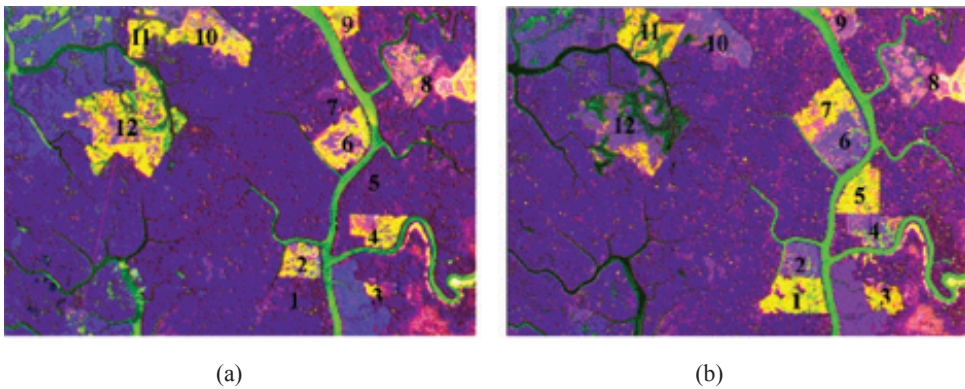


Fig. 2: Images for area 1 (a) Image dated 5th August 2005, (b) Image dated 13th June 2007

Based on the ten years' working plan (i.e. from 2000 to 2009) given by Perak Forestry Department, Matang Mangrove forest would go through two thinning processes before is being harvested. Only excellent and good forests, as well as old growth forest, would be allocated as the final feeling areas for harvesting. The forest is ready for the final feeling after five years of the second thinning process. All the allocated forests must be 30 years or older at the time of harvesting (Azahar & Nik Mohd. Shah, 2003).

In this study, four areas namely area 1, area 2, area 3, and area 4 were selected and used and these areas were also scheduled for harvesting. In total, there are 12, 9, 3, and 5 change locations which had been visually identified from the working plan map and field visits in area 1, area 2, area 3 and area 4, respectively.

Area 1

Fig. 2 shows the image of area 1 with the size of 750 x 505 pixels. In this area, 12 locations were identified as the changed areas. Descriptions of the year of harvesting in those areas are tabulated in Table 1.

TABLE 1
Detail condition of the plant in Area 1 based on the working plan for the Matang Mangrove Forest Reserve, Perak

Location number	Year of harvest (plan)	Condition in 2007 (visual inspection)
1	2004	Lost
2	2001	Growth
3	2003	Loss
4	2001	Growth
5	2005	Loss
6	2001	Growth
7	2003	Loss
8	2000	Growth
9	2002	Growth
10	2001	Growth
11	2003	Loss
12	2000	Growth

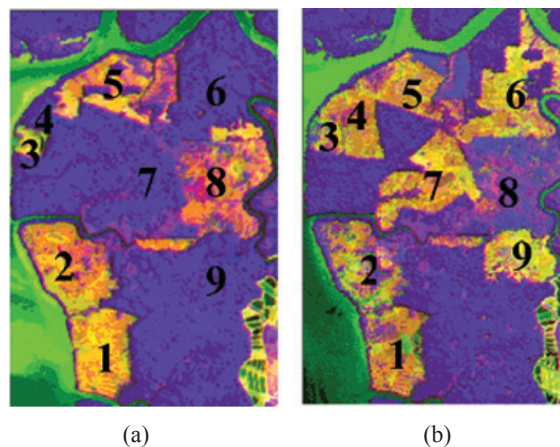


Fig. 3: Images for area 2; (a) Image dated 5th August 2005, (b) Image dated 13th June 2007

Based on the working plan given by Perak Forestry Department, the harvesting process at locations 1 and 7 should begin in 2004 and 2003, respectively. However, Fig. 2a shows that those locations were still represented by the magenta colour, indicating the forest area. According to a forest officer at Perak Forestry Department this was probably due to the delaying process of harvesting by the contractor. Fig. 2b illustrates that these areas were clearly harvested in 2007. Other mismatched conditions were detected in locations 3 and 11. Nonetheless, the working plan of Perak Forestry Department revealed that the harvesting process should begin in 2003 for both the locations. On the contrary, only parts of those areas were harvested in 2005. The targeted process was achieved for harvesting in 2007.

TABLE 2
Detail condition of the plant in Area 2, based on the working plan for the
Matang Mangrove Forest Reserve, Perak

Location number	Year of harvest (plan)	Condition in 2007 (visual inspection)
1	2003	Growth
2	2001	Growth
3	2001	Growth
4	2004	Loss
5	2003	Loss
6	2004/2005	Loss
7	2004	Loss
8	2001	Growth
9	2005	Loss

TABLE 3
Detail condition of the plant in Area 3 based on the working plan for the
Matang Mangrove Forest Reserve, Perak

Location number	Year of harvest (plan)	Condition in 2007 (visual inspection)
1	2006	Loss
2	2000	Loss
3	2003	Loss

Area 2

Fig. 3 shows image of area 2 with the size of 234 x 338 pixels. A total of nine locations were identified as the changed areas. Details and descriptions about the year of harvesting in those areas are tabulated in Table 2.

Fig. 3a compares the years of harvest in the working plan. Based on this working plan, locations 4, 6, and 7 should have been harvested in 2004. However, the satellite image illustrated in *Fig. 3a* revealed that those areas were still covered by plants. This indicates that in those areas, the process of harvesting was still not started up to 2005. On the other hand, the harvesting process in location 5 should begin in 2003. Nonetheless, the image taken in 2005 showed that this area was not fully cleared until that particular year.

Area 3

Fig. 4 shows the image of area 3 with the size of 257 x 437 pixels. For this particular area, there are three locations identified as changed areas. Descriptions of the year of harvesting in those areas are presented in Table 3.

Location 1 was scheduled to be harvested in 2006. Therefore, it can be seen in *Fig. 4a* that this particular location was still covered by plants in 2005. Meanwhile, *Fig. 4b* shows that only a small portion of location 1 was harvested in 2007. This means that the harvesting process had been started. For location 2, the map of the working plan shows that this particular area should

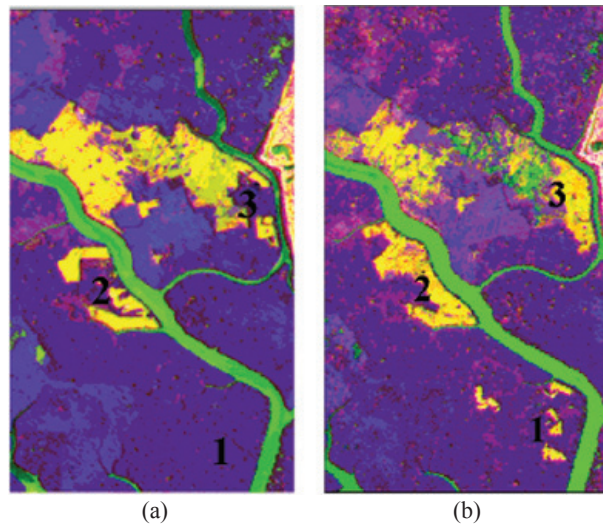


Fig. 4: Images for area 3; (a) Image dated 5th August 2005, (b) Image dated 13th June 2007

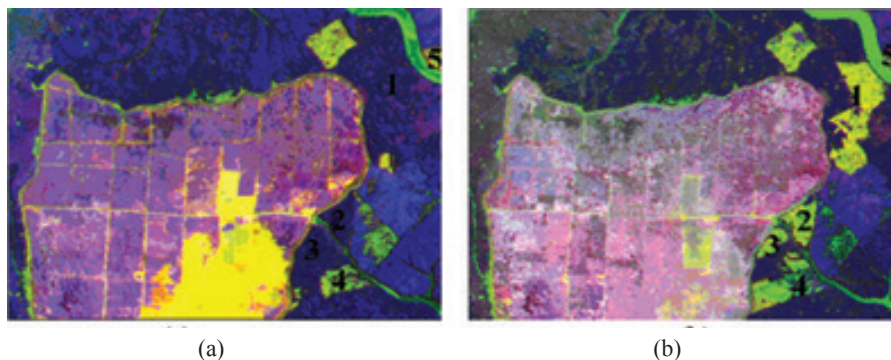


Fig. 5: Images for area 4; (a) Image dated 5th August 2005, (b) Image dated 13th June 2007

already be harvested in 2000. However, the image in *Fig. 4a* shows that this location was still not fully harvested until 2007. It took about 5 years to fully harvest this areas and this might be due to problem on the contractor's part. Meanwhile, Location 3 was supposed to be harvested in 2003. Nevertheless, the process was still not done up to 2005. This location was fully cleared only in 2007.

Area 4

Fig. 5 shows the image of area 4 with the size of 489 x 374 pixels. There were five locations considered to be changed areas. Further descriptions of the year of harvesting in those areas are mentioned in Table 4.

Fig. 5a shows that although the areas in location 1 were scheduled to be harvested in 2000, the harvesting process was not even started in locations 1, 2, 3, and 4 in 2005. However, those areas were successfully cleared in 2007, as illustrated *Fig. 5b*.

TABLE 4
Detail condition of the plant in Area 4, based on the working plan for the Matang Mangrove Forest Reserve, Perak

Location number	Year of harvest (plan)	Condition in 2007 (visual inspection)
1	2001	Loss
2	2005	Loss
3	2005	Loss
4	2004	Loss
5	2000	Growth

Location 5 was identified as a cleared area in 2005 because it was already harvested in 2000. Fig. 5b shows that some plants already started to grow in this location based on the image taken in 2007.

METHODOLOGY

Image Pre-processing

Before performing the change detection technique, the images need to be pre-processed. Pre-processing includes radiometric and geometric corrections. The radiometric correction was done by the Axis Commerce, located in Selangor, Malaysia. Therefore, the pre-processing undertaken in this study only involved a geometric correction.

Local Mutual Information

The proposed forest change detection technique was developed based on the modification of the change detection technique used to detect landslide with huge extent by Khairunniza-Bejo *et al.* (2010). Instead of detecting the huge amount of changes, the original technique was modified to detect any changes which are considered to have significant changes.

Point similarity measure is defined as a measure which is used to calculate the similarity of individual pixels. The basic idea of the method is that any change pixel value is maximally dissimilar, i.e. the value of similarity of these pixels will be low. Therefore, in this study, the location of the changes in the image of the forest areas was first detected by calculating the value of mutual information for every pixel in the images. These data were then analyzed to differentiate between the change and unchanged areas.

Mutual information of the two images over their overlapping part was computed using equation 1, as follows:

$$M_{AB} = \sum_{p^A} \sum_{p^B} P_{AB}(p_i^A, p_i^B) \log \left[\frac{P_{AB}(p_i^A, p_i^B)}{P_A(p^A)P_B(p^B)} \right] \quad (1)$$

Where, $P_A(p^A)$ is the normalized histogram of the grey values of the reference image, $P_B(p^B)$ is the normalized histogram of grey values of the sensed image, $P_{AB}(p_i^A, p_i^B)$ is the normalized joint histogram of the grey values of p_i^A and p_i^B which correspond to the same pixel, i .

Then, the local mutual information is derived from the global mutual information. Equation 1 can be written as:

$$M_{AB} = \sum_{P_A} \sum_{P_B} \frac{N_i}{N} \log \left| \frac{P_{AB}(p_i^A, p_i^B)}{P_A(p^A)P_B(p^B)} \right| \tag{2}$$

$$= \frac{1}{N} \sum_c \log \left| \frac{P_{AB}(p_c^A, p_c^B)}{P_A(p^A)P_B(p^B)} \right|$$

Where, N_i is the number of the occurrences of intensity pair, (p_i^A, p_i^B) and N is the number of pixels in the overlapping part of the two images. Meanwhile, $P_{AB}(p_c^A, p_c^B)$ is the normalized joint histogram of the grey values, p_c^A and p_c^B , which correspond to the same coordinate, c .

The final summation was taken over the spatial image coordinates instead of the intensities. Therefore, the global similarity can be treated as an average of the point similarities defined for each pixel at coordinate, c :

$$M_{AB} = \frac{1}{N} \sum_c SM_{AB} \tag{3}$$

where

$$SM_{AB} = \log \left[\frac{P_{AB}(p_c^A, p_c^B)}{P_A(p^A)P_B(p^B)} \right] \tag{4}$$

The point similarity of a pixel in each coordinate was also calculated. Thus, every pixel in location c is represented by its value of mutual information. After that, the local mutual information image was threshold, as follows:

$$G(c) = \begin{cases} 0 & \text{if } SM_{AB} > Th \\ 255 & \text{if } SM_{AB} \leq Th \end{cases} \tag{5}$$

Where, Th is the threshold value and $G(c)$ is the binary value of the pixel at the coordinate c in the threshold image. Therefore, the changed areas are represented by the white pixels in a binary image.

Normalized Differenced Vegetation Index (NDVI)

The Normalized Differenced Vegetation Index (NDVI) presents the amount of photosynthesizing vegetation. The NDVI is calculated using spectral reflectance measurements acquired in the red and near-infrared regions. It is based on the band rationing, and calculated from the individual measurements, as follows:

$$NDVI = \frac{(NIR - RED)}{NIR + RED} \tag{6}$$

The change areas were then detected from the different NDVI images.

Image Differencing

Image differencing requires each pixel value in the image to be subtracted from its corresponding pixel value in the other image. This particular technique is simple, straightforward, and easy

to interpret the result method. However, it cannot provide a detailed change matrix. The most challenging part in using this particular technique lies in the selection of the threshold value. In more specific, the technique requires a trial and error process in order to get the best threshold value.

Accuracy Assessment

The accuracy of the results given by all of the change detection techniques was also compared. The accuracy was verified using the field data provided by the working plan for Matang Mangrove Forest, Perak, by Perak Forestry Department. The total number of pixel for the changed area which varied in all technique was compared with the real total number of pixels which was stated in the working plan. This was done by overlapping the reference image with the results given by the change detection technique. Therefore, the percentage of accuracy is calculated as follows:

$$\% \text{ Accuracy} = \frac{G_d}{G_f} \times 100 \quad (7)$$

where G_d is the total pixel detected from the change detection technique and G_f is the total pixel from the field data.

RESULTS AND DISCUSSION

Image Pre-processing

Geometric correction was done during the image pre-processing stage. It is a process of finding the best fit between the sensed image and the reference image. As a result, the pixel at location A in the sensed image has the same meaning with the pixel at the same location in the referenced image. In this study, the image taken on 5th August 2005 and 13th June 2007 was used as a referenced and a sensed image, respectively. The steps involved in geometric corrections include locating Ground Control Points (GCPs) and image resampling. Fifty GCPs, namely, water body, the intersection of river and road were identified from both the images. These GCPs were widely dispersed throughout the images and used to correct the geometric distortion in an image by matching the coordinates of the images with those of the map. Each GCP was ordered by the residual error it contributed to the polynomial fit. It is calculated as follows:

$$RMSE = \sqrt{(x_1 - x_0)^2 + (y_1 - y_0)^2} \quad (8)$$

Where, x_0 and y_0 are the original image column and row coordinates of the GCP, whereas x_1 and y_1 are the computed original image column and row coordinates of the GCP, respectively. The first order transformation was used in the experiment. Image fit was considered acceptable if the root means square (RMS) error is less than half pixel width, i.e. $RMSE < 0.5$ pixels. In this study, the average value for both the images was calculated as 0.34, which is acceptable.

After the GCPs had been collected, the next step of geometric correction was the re-sampling process. Re-sampling involved interpolating between the existing pixels to obtain and estimate their values in the new pixel locations. In this study, the nearest neighbour interpolation technique was used during the re-sampling process. Therefore, the pixel value which is closest to the new pixel location (x', y') is assigned to the output pixel location (x, y) (Jensen, 1996). This particular technique was selected because of its simplicity and capability to retain colour information of the image. Therefore, it is computationally efficient. Besides, the technique enlarges a digital image for the purpose of closer examination.

Local Mutual Information

Figs. 6a, b, c, and d show the histogram distribution of the values of the local mutual information calculated in area 1, i.e. between the images taken on 5th August 2005 and 13th June 2007 for band 1, band 2, band 3, band 4, respectively. The figures show that the mutual information image is dominated by zero to one mutual information value. After locating the value of the local mutual information in every pixel location, the images need to be threshold by using a trial and error process. This was done to classify the changed and unchanged areas.

The changed areas were identified with the threshold values of 1, 0 and -1, as shown in Figs. 7, 8 and 9, respectively. The changed areas in these figures are represented by the white pixels. Therefore, if the threshold value of 1 was chosen, pixel with the value of local mutual information greater than 1 would be eliminated. These pixels are defined as the unchanged areas. Fig. 7a shows the results for the detected changed area in band 1 by using a threshold value of 1. From this figure, it is clear that most of the areas are recognized as the changed areas. The same condition was also found in the images for band 2, band 3 and band 4. When the threshold value decreased to zero (Fig. 8), it could be seen that the areas which had been detected as the changed areas would be the same as what was seen by our eyes; similar thing was found in the map given by Perak Forestry Department. Meanwhile, Figs. 8a, b, c, and d show the results for band 1, band 2, band 3, and band 4 images, respectively. When the threshold value reduced to negative one (Fig. 9), i.e. only the pixel values of the negative one and below were identified as changes, less changed areas were detected, as shown in Fig. 9a. From Figs. 7 to 9, it can be seen that the threshold value of 0 is more appropriate to differentiate between the changed and unchanged areas in all the band images. Therefore, it can provide solution on the trial and error processes of selecting a threshold value. The local mutual information images were threshold as follows:

$$G(c) = \begin{cases} 255 & \text{if } S_{M_{AB}} > 0 \\ 0 & \text{if } S_{M_{AB}} \leq 0 \end{cases} \quad (9)$$

Where, $S_{M_{AB}}$ is the average point similarity and $G(c)$ is the binary value of the pixel at coordinate c in the threshold image. The changed areas are represented by the white pixels in a binary image. The same conditions were also observed for the other areas.

Fig. 8 shows the result of the local mutual information for area 1 using a threshold value of 0. From this figure, it can be seen that in general, band 2, band 3, and band 4 could clearly identify the changes, especially in locations 1, 3, 5, and 7. The results for band 1, nonetheless, could not give a clear classification of the changed and unchanged areas. In other words, the change and unchanged regions could not be clearly isolated, specifically at the border of the regions.

However, in general, the results from certain bands are still not promising. Therefore, the results of change detection in every band would be analyzed to identify the band with the best results. The results for the local mutual information were then compared with those of the map of a working plan for the Matang Mangrove Forest Reserve, Perak. Table 1 shows details of the condition detected in the location in area 1.

Figs. 8b, c, and d show that band 2, band 3, and band 4 gave quite similar results of change detection. In particular, band 1 (see Fig. 8a) could not clearly differentiate between the changes and unchanged areas. As for locations 5, 7, and 1, the regions of change and unchanged could be clearly isolated, especially at the border of the region. Fig. 8b reveals that band 2 could detect

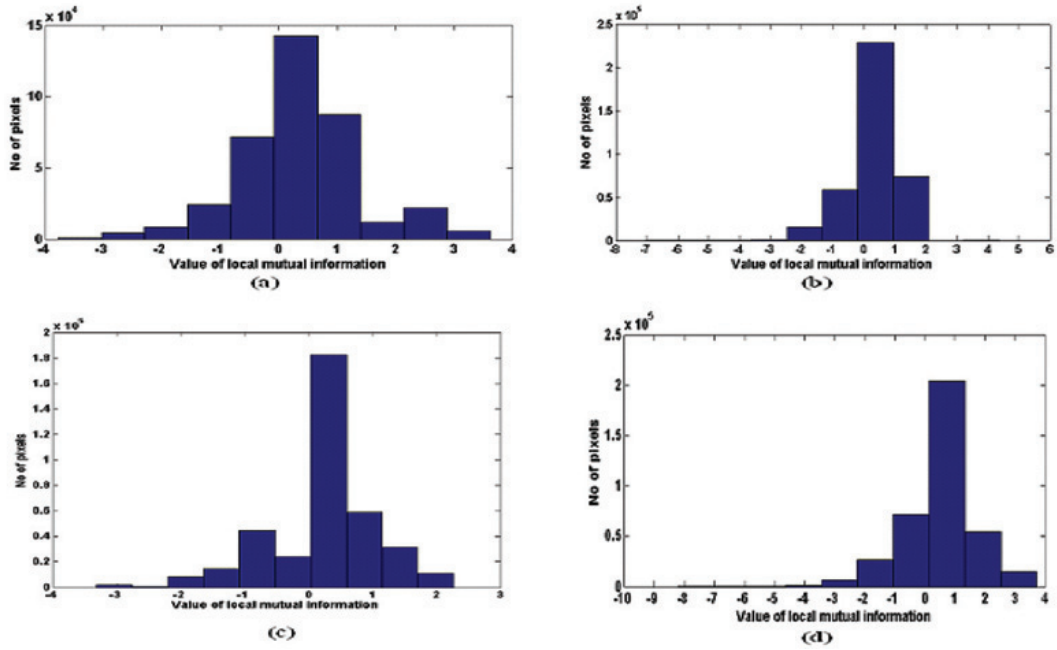


Fig. 6: Histogram distribution of the value of the local mutual information calculated in area 1; (a) Band 1 (b) Band 2 (c) Band 3 (d) Band 4

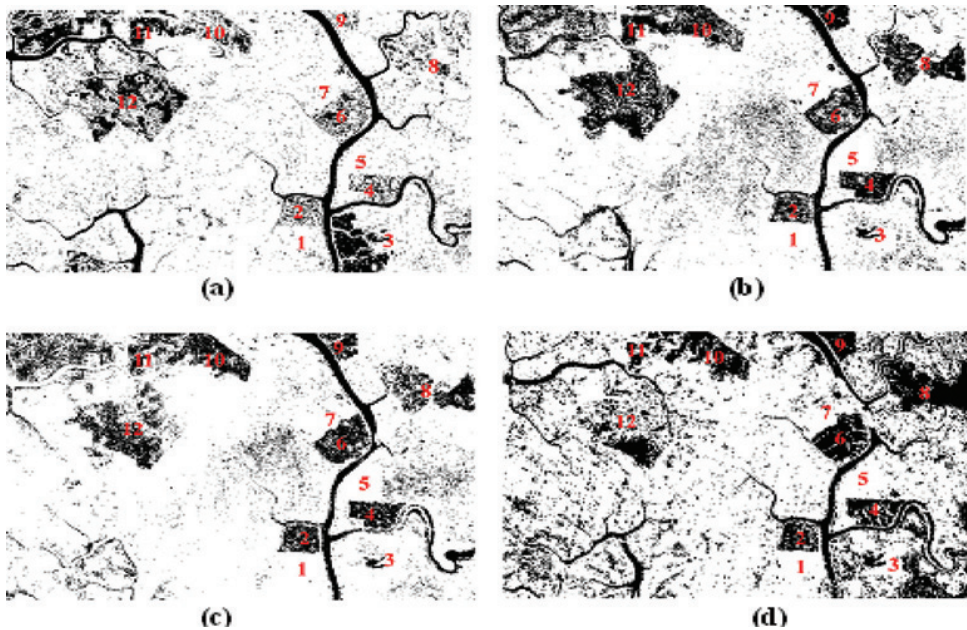


Fig. 7: Result of the mutual information for area 1 using thresholding the value of 1. Changed areas are shown in white pixels and unchanged ones are represented by black pixels. (a) Changed areas for Band 1, (b) Changed areas for Band 2, (c) Changed areas for Band 3, (d) Change areas for Band 4

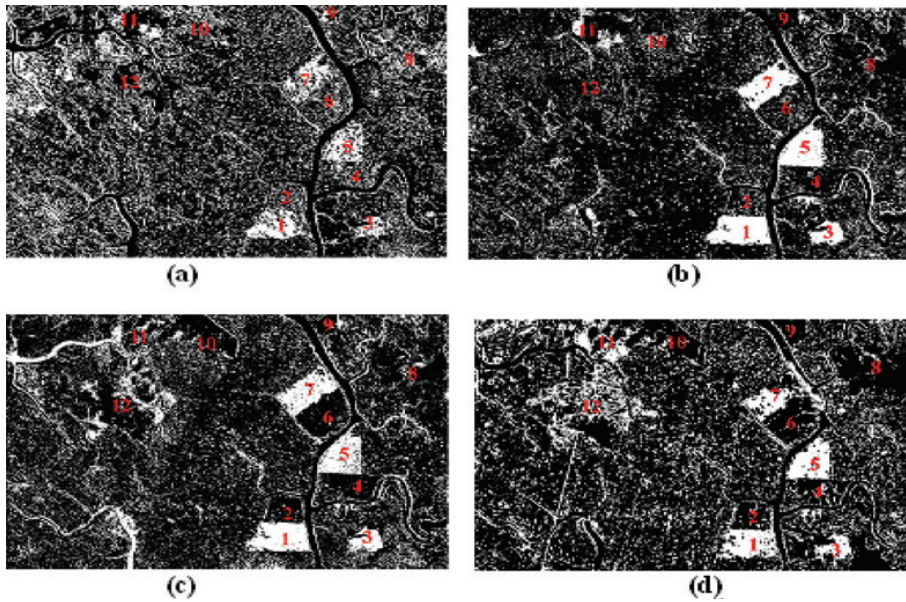


Fig. 8: Result of mutual information for area 1 using thresholding value of 0. Change areas are shown in white pixels and unchanged are represented by black pixels. (a) Change areas for Band 1, (b) Change areas for Band 2, (c) Change areas for Band 3, and (d) Change areas for Band 4

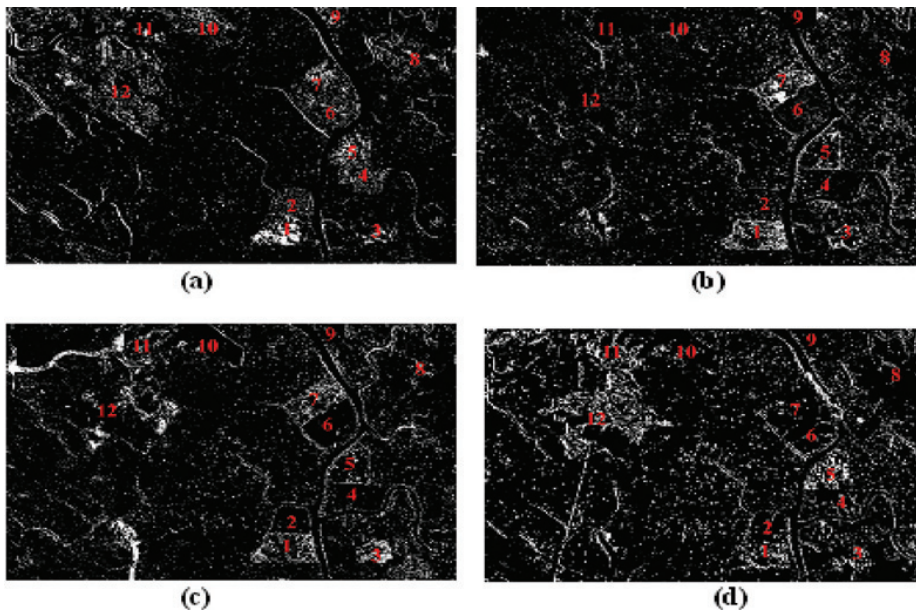


Fig. 9: Result of the mutual information for area 1 using the thresholding value of -1. Changed areas are shown in white pixels and unchanged areas are represented by black pixels. (a) Changed areas for Band 1, (b) Changed areas for Band 2, (c) Changed areas for Band 3, and (d) Changed areas for Band 4

changes at locations 1, 3, 5, 7, and 11, which were also identified as the loss areas. The growth area in locations 2, 4, 6, 10, and 12 are mixed with the white and black pixels.

The results gathered for band 3 and band 4 are shown in *Fig. 8c* and *8d*, respectively. Even though the white pixel can only be used to detect the loss areas, which are at locations 1, 5, 7, and 3, the growth areas at locations 2, 4, 6, 8, 9, 10, and 12 are clearly represented by black colour. This also means that the local mutual information in those areas is greater than zero and has the same group with those in the unchanged areas.

Table 2 shows a detailed condition of the plant in area 2 based on the working plan for the Matang Mangrove Forest Reserve, Perak. *Figs. 10a, b, c, and d* show the results for the local mutual information using the threshold value of 0 for area 2 in bands 1, band 2, band 3 and band 4, respectively. From these figures, it can be seen that band 2 and band 3 give quite similar results.

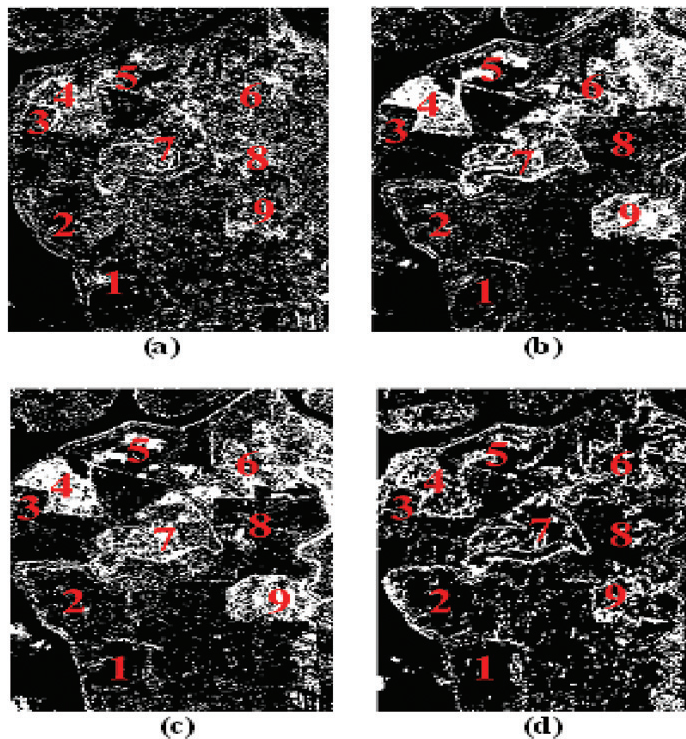


Fig. 10: Result of the mutual information for area 2, using thresholding value of 0. Changed areas are shown in the white pixels and the unchanged areas are represented by the black pixels. (a) Changed areas for Band 1, (b) Changed areas for Band 2, (c) Changed areas for Band 3, and (d) Changed areas for Band 4

There are five lost areas in area 2 (i.e. in locations 4, 5, 6, 7, and 9, respectively), as depicted in Table 2. These areas were detected as the changed areas and represented by the white pixels. The growth areas are located in locations 1, 2, 3, and 8. Since the growing condition is also defined as the changed conditions, these locations should therefore be represented by white pixels. However, the results presented in *Fig. 10* show that the growth areas are represented by the black pixels. It means that the growth areas were grouped into the unchanged areas. Overall, the results show that the loss and growth areas can easily be isolated using band 2 and band 3. Both bands can clearly

identify the changed areas. Compared to the results for band 4 in which all changed locations could be detected, it cannot cover the whole changed areas, and only the edge of the growth areas could be detected. For the loss location, on the other hand, the whole change areas were fully covered.

Table 3 shows a working plan of the Matang Mangrove Forest reserve, Perak for area 3. From the table, location 1 was planned to be harvested in year 2006, whereas location 2 in 2000 and location 3 in 2003. The image taken in 2005 (*Fig. 4a*), however, shows that there are still some forest areas in locations 2 and 3, as indicated by the magenta colour. According to the Forest Officer, the harvesting process might be delayed in certain areas. However, both the locations were successfully harvested in 2007, as shown in *Fig. 4b*. Therefore, the growth condition was assumed in both locations in 2007 because a gap of more than four years than the planned harvesting time is not applicable. The results for band 2 (*Fig. 11b*) and band 3 (*Fig. 11c*) are more acceptable than those of band 1 (*Fig. 11a*) and band 4 (*Fig. 11d*). In band 2 and band 3, all of the lost locations could be detected by the local mutual information. Those areas are represented by the white pixels. Both the bands gave quite similar results.

The detailed conditions for area 4, based on the working plan for the Matang Mangrove Forest Reserve, Perak, are given in Table 4. Location 1 of area 4 was planned to be harvested in 2001. However, there were still some forest areas in location 1 in 2005, as shown in *Fig. 5a*. *Fig. 5b* shows that this area was successfully harvested in 2007. Therefore, location 1 has been identified as a loss of plant condition. Band 3 (*Fig. 12c*) and band 4 (*Fig. 12d*) yielded the same results, as what had been expected. Both the bands could detect all the changed areas caused by plant loss in locations 1, 2, 3, and 4. Meanwhile, *Fig. 12b* shows that band 2 could only detect the edge of the changed locations, whereas band 1 (*Fig. 12a*) gave a totally different result. It could not detect the loss and growth areas at all.

Overall, the use of the local mutual information in forest monitoring is promising. It could successfully detect changes caused by plant loss. However, further analysis is still needed to identify the changes caused by plant growth. Band 2 and band 3 gave quite similar results in all the areas. Both bands clearly identified the changed areas. Therefore, it can be concluded that band 2 and band 3 are the best bands to be used in change detection for forest areas using the local mutual information technique, as compared to the other bands (band 1 and band 4).

Image Differencing

Fig. 13 shows a histogram distribution of the distinguished images. The best threshold for the changed areas was determined using the trial and error technique. The figure shows that the graphic representations of image differencing pixel distribution are skewed to the right of the histogram. Meanwhile, the pixel values varied from 0 to 50.

Four different threshold values, namely, 50, 100, 125 and 150, were used in this study. The best threshold value was selected based on its capability to detect the changed areas. The results from the experiment show that a threshold value of 50 can detect changes in area 1 in all the bands, as illustrated in *Fig. 14*. This threshold value, nevertheless, is not applicable to all the bands of the other areas. Table 5 shows a summary of the best threshold value for each area in all the bands. Normalized Differenced Vegetation Index

The value of NDVI varies between -1.0 and +1.0. The vigorously growing healthy vegetation has low red-light reflectance and high near-infrared reflectance. Therefore, it produces high NDVI values. The mounting amount of the positive NDVI values indicates the increasing amounts of green vegetation. Meanwhile, the NDVI values near zero and decreasing negative values indicate non-vegetated features, such as barren surfaces (rock and soil) and water, snow, ice, and clouds. In this study, the NDVI data were re-scaled to 0-255 so as to store the results as unsigned 8-bit data.

TABLE 5
Summary of the best threshold value for image differencing technique

Area	Band	Threshold value
1	Band 1	50
	Band 2	50
	Band 3	50
	Band 4	50
2	Band 1	50
	Band 2	50
	Band 3	50
	Band 4	50
3	Band 1	100
	Band 2	150
	Band 3	125
	Band 4	100
4	Band 1	100
	Band 2	150
	Band 3	100
	Band 4	100

TABLE 6
Summary of the best threshold value for difference of NDVI technique

Area	Threshold value
1	125
2	140
3	125
4	130

TABLE 7
Accuracy statistics for change detection techniques

Area	Local mutual information	Image differencing	NDVI
1	40.55%	58.33%	46.42%
2	31.97%	53.20%	45.85%
3	51.85%	55.39%	95.92%
4	81.07%	51.32%	80.79%

The re-scaled process was done using the following equation:

$$I(n) = \frac{|X(n) - \bar{X}|}{|X_{Max} - X_{min}|} \times 255 \quad (10)$$

where $I(n)$ is the scaled image, $X(n)$ is the value of NDVI of n , \bar{X} is the mean value, X_{Max} is the maximum value of NDVI, X_{Min} is the minimum value of NDVI. The scaled NDVI image taken on 13th June 2007 was then subtracted to the scale NDVI image of 5th August 2005. The histogram distribution of the different images is shown in *Fig. 15a*. The histogram will be used as a guideline

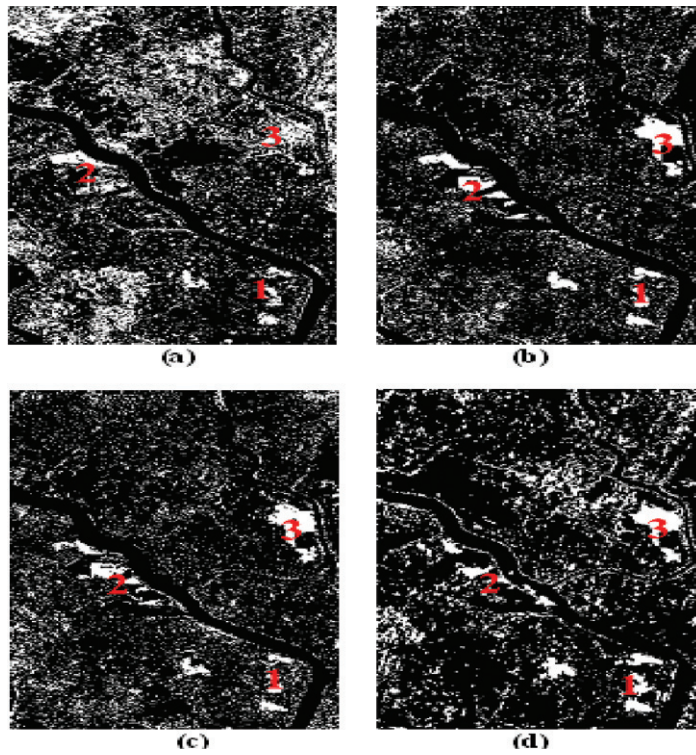


Fig. 11: Result of the mutual information for area 3, using the thresholding value of 0. Changed areas are shown in the white pixels and the unchanged areas are represented by the black pixels. (a) Changed areas for Band 1, (b) Changed areas for Band 2, (c) Changed areas for Band 3, and (d) Changed areas for Band 4

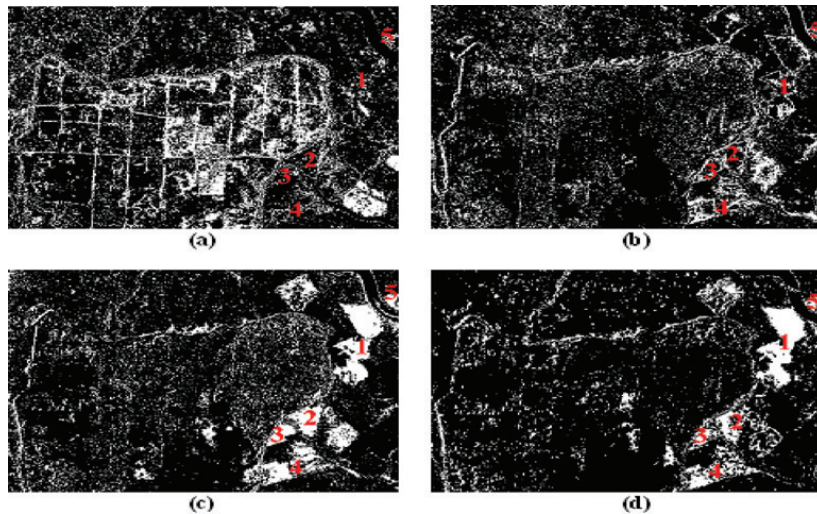


Fig. 12: Result of the mutual information for area 4 using the thresholding value of 0. Changed areas are shown in the white pixels and unchanged areas are represented by the black pixels. (a) Changed areas for Band 1, (b) Changed areas for Band 2, (c) Changed areas for Band 3, and (d) Change areas for Band 4

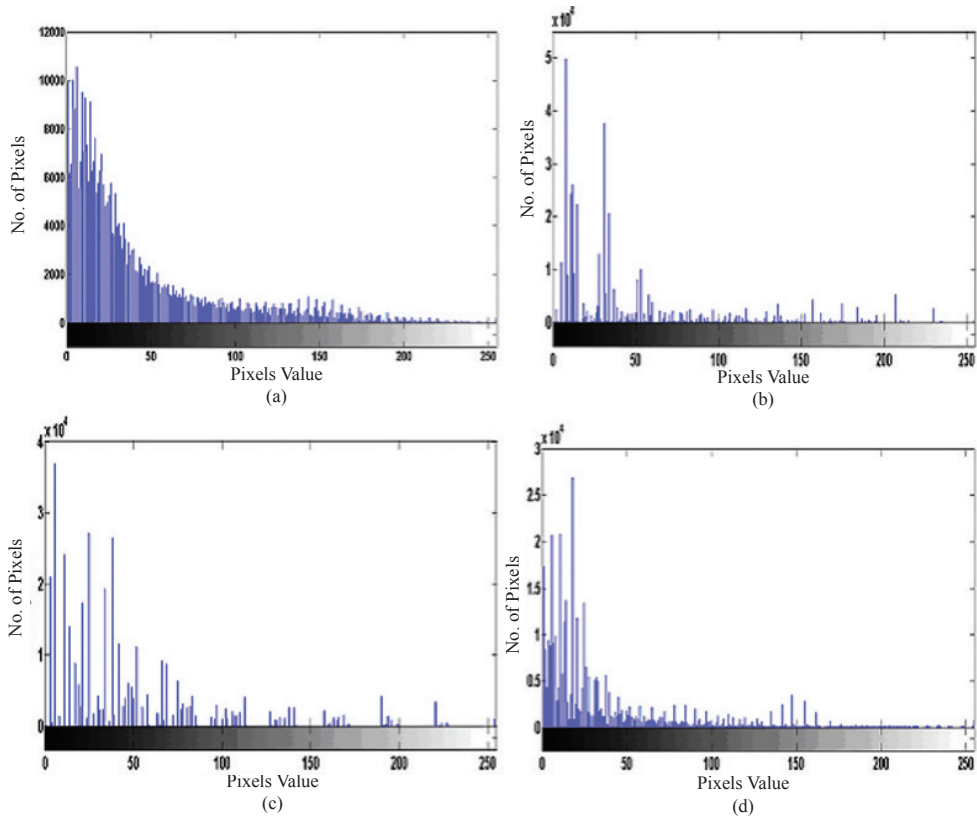


Fig. 13: Histogram distribution of the value of image differencing calculated in area 1; (a) Band 1, (b) Band 2, (C) Band 3, and (d) Band 4

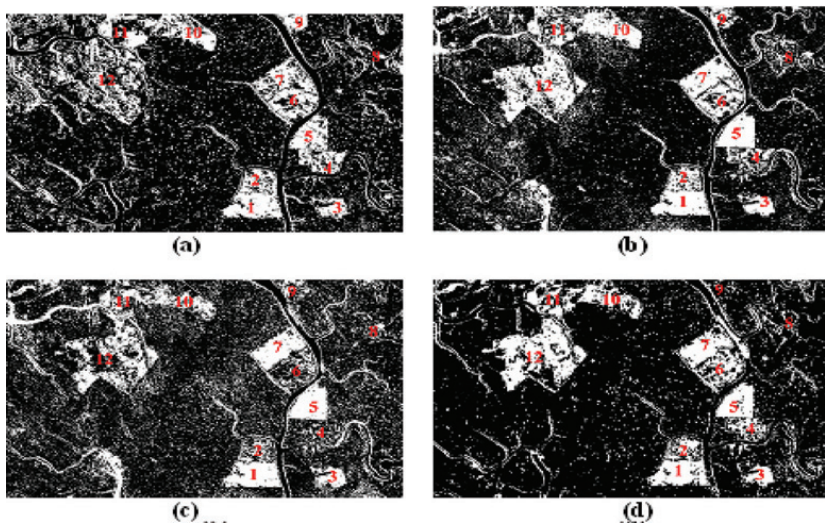


Fig. 14: Result of image differencing for area 1 with the threshold value of 50. Changed areas are shown in the white pixels and unchanged areas are represented by the black pixels; (a) Band 1, (b) Band 2, (C) Band 3, and (d) Band 4

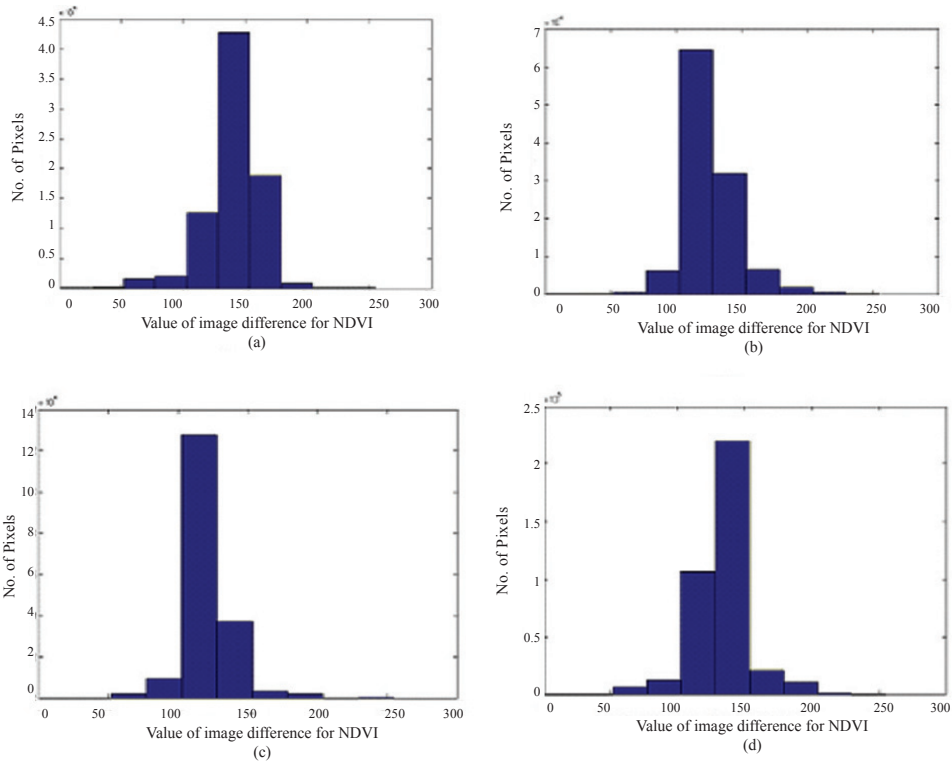


Fig. 15: Histogram distribution of the value of image differencing for NDVI; (a) Area 1, (b) Area 2, (c) Area 3, and (d) Area 4

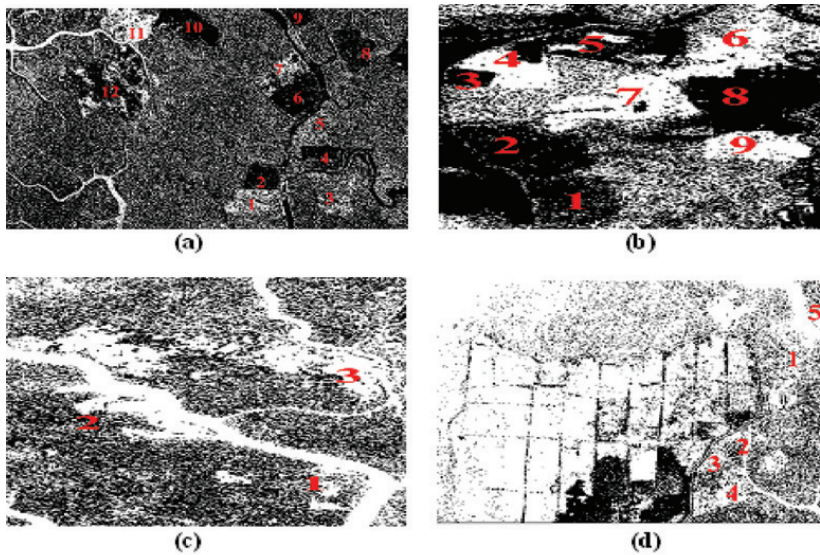


Fig. 16: Result of the change detection for NDVI using the best threshold value. Changed areas are shown in the white pixels and unchanged areas are represented by the black pixels; (a) Area 1 with the threshold value of 125, (b) Area 2 with the threshold value of 140, (c) Area 3 with the threshold value of 125, and (d) Area 4 with the threshold value of 130

in selecting a threshold value. The threshold values of 125, 130, 135, and 140 were used during the trial and error process. The best threshold value in every area is tabulated in Table 6. From this table, it can be seen that the best threshold value is not the same for all the areas. The results for the detected change areas are shown in *Fig. 16*. Overall, the result of the NDVI after the thresholding process is quite similar to those of the simple local mutual information. It can only detect the change areas caused by plant loss. The changed areas caused by plant growth are grouped into unchanged condition.

Accuracy Assessment

The results for the local mutual information, image differencing and NDVI were compared with those of the reference image, based on the map in the working plan of Matang Mangrove Forest, Perak, taken from Perak Forestry Department (Azahar & Nik Mohd. Shah, 2003). This was done by overlapping each of them with the reference image. The accuracies of the results in each technique were then computed and compared.

The percentages of the overlapping pixels in all the techniques were calculated to determine their accuracy. Table 7 shows the accuracy of each technique in all the studied areas. From the table, it can be seen that image differencing can accurately detect the location of the changes at two out of the four areas, with the percentage accuracy of 58.33% and 53.20% for area 1 and area 2, respectively. NDVI gives the highest percentage of accuracy (95.92%) in area 3. The local mutual information shows a higher percentage of accuracy in area 4, with 81.07%.

CONCLUSION

In this study, three different techniques of change detection were used to detect the changes in Matang Mangrove Forest areas. Although the image differencing technique has given the highest percentage of accuracy in 2 out of the 4 areas undertaken in the study, the value of its percentage of accuracy is rather small (i.e. less than 60%). Both difference NDVI and local mutual information techniques successfully detected the changes in 2 other areas, with higher percentages of accuracy, namely, 95.92% (area 3) and 81.07% (area 4), respectively. Hence, it can be concluded that both the techniques perform better in less growth condition areas – as tabulated in Tables 4 and 3, where the numbers of growth locations were identified as 1 out of 5 in area 4 and none in area 3. Meanwhile, the number of growth locations was identified as 7 out of 12 in area 1 (Table 1) and 4 out of 9 in area 2 (Table 2). The consistency of the best threshold value in detecting changes gives the advantage to the local mutual information technique. However, the pure local mutual information technique, which does not adopt any morphological operations in detecting changes, still needs to be refined to make it more applicable for use in forest areas. This can be done by analyzing the value of the mutual information in plant growth areas compared to the value of the local mutual information in the unchanged areas.

Moreover, it can be concluded that band 3, which is sensitive to vegetation biomass, gave the best results in all the conditions for change detection as compared to the other bands. Therefore, the use of only a single band for change detection operation not only can help the reduction of memory allocation, but also reduces the time taken to process the image.

ACKNOWLEDGEMENTS

The authors wish to thank and are grateful to the Perak Forestry Department for providing the working plan of the Matang Mangrove Forest, Perak and appropriate field visits for us. This work was supported by Fundamental Grant (FRGS), project number 02-01-07-040FR.

REFERENCES

- Alberga, V. (2009). Similarity measures of remotely sensed multi-sensor images for change detection applications. *Remote Sensing*, 1, 122-143.
- Alongi, D. M. (2002). Present state and future of the world's mangrove forests. *Environmental Conservation*, 29, 331-349.
- Azahar Muda, & Nik Mohd. Shah. (2003). *A working plan for the Matang Mangrove Forest Reserve, Perak*. Perak: State Forestry Department of Perak Darul Ridzuan.
- Bosire, J. O., Dahdouh-Guebas, F., Walton, M., Crona, B. I., Field, C., Kairo, J. G., *et al.* (2008). Functionality of restored mangroves: A review. *Aquatic Botany*, 89, 251-259.
- Conchedda, G., Durieux, L., & Mayaux, P. (2008). An object-based method for mapping and change analysis in mangrove ecosystems. *ISPRS Journal of Photogrammetry & Remote Sensing*, 63, 578-589.
- Coppin, P. R., & Bauer, M. E. (1994). Processing of multitemporal landsat TM imagery to optimise extraction of forest cover change features. *IEEE Transactions on Geoscience and Remote Sensing*, 32, 918-927.
- Danielsen, F., Sørensen, K.M., Olwig, M. F., Vaithilingam Selvam, Faizal Parish, Burges, N. D., *et al.* (2005). The Asian tsunami: A protective role for coastal vegetation. *SCIENCE*, 310, 643.
- FAO. (2007). Forestry reporting requests. *Food and Agriculture Organization of the United Nations, Rome, Italy*. 23, 5-67.
- Guild, L. S., Cohen, W. B., & Kauffman, J. B. (2004). Detection of deforestation and land conversion in Rondonia, Brazil using change detection techniques. *International Journal of Remote Sensing*, 25(4), 731-750.
- Hayes, J. D., & Sader, S. A. (2001). Comparison of change detection techniques for monitoring tropical forest clearing and vegetation regrowth in a time series. *Photogrammetric: Engineering & Remote Sensing*, 67, 1067-1075.
- Howari, F. M., Jordan, B. R., Bouhounce, N., & Wyllie-Echeverria, S. (2009). Field and remote-sensing assessment of mangrove forests and seagrass beds in the Northwestern Part of the United Arab Emirates. *Journal of Coastal Research*, 25(1), 48-56.
- Inglada, J. (2002). Similarity measure for multisensor remote sensing Images. *Remote Sensing*, 104-106.
- Jensen, J.R. (1996). *Introductory digital image processing: A remote sensing perspective* (2nd ed.). Upper Saddle River, N.J.: Prentice Hall.
- Khairunniza-Bejo, S., Petrou, M., & Ganas, A. (2010). *Local similarity measure for landslide detection and identification in comparison with the image differencing method*. *International Journal of Remote Sensing*, 31(23), 6033-6045.
- Lee, T. M., & Yeh, H. C. (2009). Applying remote sensing techniques to monitor shifting wetland vegetation: A case study of Danshui River Estuary Mangrove Communities, Taiwan. *Ecological Engineering*, 35, 487-496.
- Liu, K., Li, X., *et al.* (2008). Monitoring mangrove forest changes using remote sensing and GIS data with decision-tree learning wetlands. *The Society of Wetland Scientists*, 28(2), 336-346.
- Lu, D., Mausel, P., Brondizio, E., & Moran, E. (2004). Change detection techniques. *International Journal of Remote Sensing*, 25(12), 2365-2407.
- Murray, M. R., Zisman, S. A., Furley, P. A., Munro, D. M., Gibson, J., Ratter, J., *et al.* (2003). The mangroves of Belize Part 1. Distribution, composition and classification. *Forest Ecology and Management*, 174(1-3), 265-279.

- Nagelkerken, I., Blaber, S. J. M., Bouillon, S., Green, P., Haywood, M., Kirton, L. G., *et al.* (2008). The habitat function of mangroves for terrestrial and marine fauna: A review. *Aquatic Botany*, 89, 155–185.
- Podeh, S. S., Oladi, J., Pormajidian, M R., & Zadeh, M. M. (2009). Forest change detection in the north of Iran using TM/ETM+ imagery. *Asian Journal of Applied Sciences*, 2(6), 464-474.
- Sader, S. A., Hayes, D. J., Hepinstall, J. A., Coan, M., & Soza, C. (2001). Forest change monitoring of a remote biosphere reserve. *International Journal of Remote Sensing*, 22(10), 1937–1950.
- Sheridan, P., & Hays, C. (2003). Are mangroves nursery habitat for transient fishes and decapods? *Wetlands*, 23(2), 449–458.